Inorganic Chemistry

Article

pubs.acs.org/IC

# Syntheses, Crystal Structures, and Magnetic Properties of Four New Cyano-Bridged Bimetallic Complexes Based on the *mer*-$[Fe^{III}(qcq)(CN)_3]^-$ Building Block

Xiaoping Shen,*[,†] Hongbo Zhou,[†] Jiahao Yan,[†] Yanfeng Li,[†] and Hu Zhou[‡]

[†]School of Chemistry and Chemical Engineering, Jiangsu University, 301, Xuefu Road, Zhenjiang 212013, China

[‡]School of Material Science and Engineering, Jiangsu University of Science and Technology, Zhenjiang 212003, China

Supporting Information

**ABSTRACT:** Four new cyano-bridged bimetallic complexes, $[\{Mn^{III}(salen)\}_2\{Fe^{III}(qcq)(CN)_3\}_2]_n\cdot 3nCH_3CN\cdot nH_2O$ (**1**) [salen = *N*,*N*′-ethylenebis(salicylideneiminato) dianion; $qcq^-$ = 8-(2-quinoline-2-carboxamido)quinoline anion], $[\{Mn^{III}(salpn)\}_2\{Fe^{III}(qcq)(CN)_3\}_2]_n\cdot 4nH_2O$ (**2**) [salpn = *N*,*N*′-1,2-propylenebis(salicylideneiminato)dianion], $[\{Mn^{II}(bipy)(CH_3OH)\}\{Fe^{III}(qcq)(CN)_3\}_2]_2\cdot 2H_2O\cdot 2CH_3OH$ (**3**) (bipy = 2,2′-bipyridine), and $[\{Mn^{II}(phen)_2\}\{Fe^{III}(qcq)(CN)_3\}_2]\cdot CH_3CN\cdot 2H_2O$ (**4**) (phen = 1,10-phenanthroline) have been synthesized and characterized both structurally and magnetically. The structures of **1** and **2** are both unique 1-D linear branch chains with additional structural units of $\{Mn^{III}(salen/salpn)\}\{Fe^{III}(qcq)(CN)_3\}$ dangling on the sides. In contrast, **3** and **4** are cyano-bridged bimetallic hexanuclear and trinuclear clusters, respectively. The intermolecular short contacts such as $\pi-\pi$ interactions and hydrogen bonds extend **1**−**4** into high dimensional supermolecular networks. Magnetic investigation reveals the dominant intramolecular antiferromagnetic interactions in **1**, **3**, and **4**, while ferromagnetic and antiferromagnetic interactions coexist in **2**. Alternating current measurement at low temperature indicates the existence of slow magnetic relaxation in **1** and **2**, which should be due to the single ion anisotropy of $Mn^{III}$.

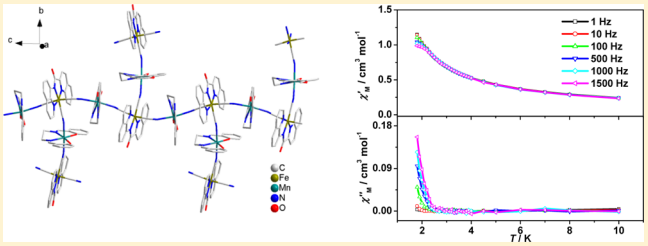


## INTRODUCTION

Low-dimensional magnets have been the hot topic in the last two decades due to their potential applications in molecular devices, high-density information storage, and quantum computers, etc.[1] The single molecule magnet (SMM) behaves as a nanomagnet under a certain temperature because of the energy barrier for reversing the magnetization derived from a large ground state spin ($S_T$) and strong easy-axis anisotropy ($D$).[2] Similar to a SMM, a single chain magnet (SCM) also exhibits slow magnetic relaxation at low temperatures because of large uniaxial anisotropy and strong intrachain exchange interactions without spin compensation between the high-spin magnetic units.[3,4] The ultimate goal of this research field is obviously to design new low-dimensional magnets, and enhance their blocking temperature ($T_B$) as high as possible.

For the design of new low-dimensional magnets, coordination complexes, especially the cyano-bridged bimetallic systems, have been attracting much attention due to their excellent magnetic properties.[5−7] Recently, modified hexacyanometalates $[(L)M(CN)_p]^{q-}$ (M = Fe, Cr; L = blocking group) have been proven to be suitable building blocks for constructing low-dimensional magnetic complexes.[8−10] The introduction of organic ligands into the cyanometalates facilitates tuning the architectures and topologies of the target complexes so that an ideal magnetic system can be designed: (i) The tailored organic ligands make the self-assembly reactions more controllable, limit the oligomerization or polymerization effect by partially blocking the coordination sites around hexacyanometalates, and promote the formation of the low-dimensional structures. (ii) The molecular geometry of blocking group L defines the molecular orbitals describing the unpaired electrons in paramagnetic centers and affects greatly the coupling mechanism, providing the valuable opportunity for chemists to tune the magnetic properties. (iii) The demand for electronic effects, steric effects, and solubility properties of the derived complexes can be readily achieved by selecting proper blocking ligands. To date, the modified hexacyanometalates that are heavily investigated are tricyanidoferrate, $[Fe^{III}(L)(CN)_3]^-$, and a great number of related magnetic assemblies have been reported.[11−14] However, to the best of our knowledge, most of the blocking ligands explored are facially coordinated to central iron ions, and the meridionally capped ones are relatively rarely reported. Recently, several new *mer*-tricyanidoferrate building blocks (Scheme 1a) employing the blocking ligands such as bis(2-pyridylcarbonyl)amidate anion (bpca),[11g,12b] 8-(pyridine-2-carboxamido)quinoline (pcq),[12c] 8-(pyrazine-2-carboxamido)quinoline (pzcq),[12d] and 8-(5-methylpyrazine-2-carboxamido)quinoline (mpzcq)[12e] have been designed and used to construct new low-dimensional

**Received:** July 8, 2013
**Published:** December 18, 2013

**Scheme 1. (a) Meridionally Coordinated Blocking Groups in $[Fe^{III}(L)(CN)_3]^-$ Anions and (b) $[Mn^{III}$(salen-type)$]^+$ Cations**

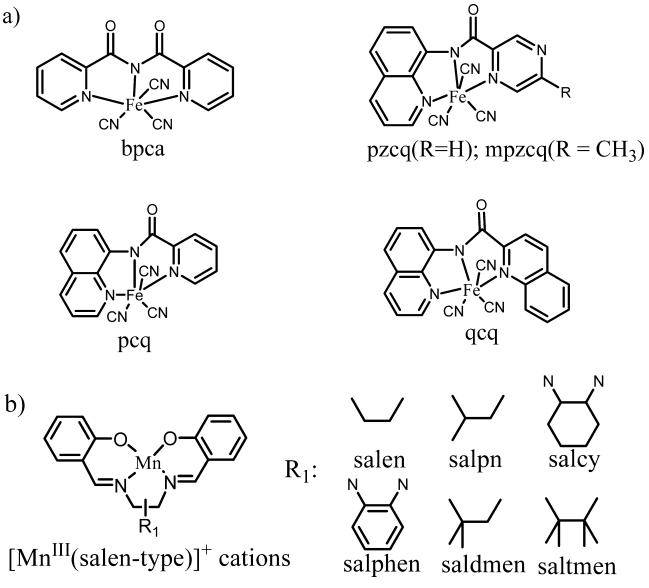


complexes. The results suggest that *mer*-tricyanidoferrate building blocks could be the next hot research topic in cyanide magnetism chemistry. In this research, we focus on the magnetic assemblies based on a recently reported *mer*-tricyanidoferrate building block of $[Fe^{III}(qcq)(CN)_3]^-$[12f] (Scheme 1a), which has been shown as a promising building block for constructing low dimensional magnets. Because $[Mn^{III}$(salen-type)$]^+$ cations (Scheme 1b) always show high spin values and large uniaxial magnetic anisotropy,[15] our synthetic strategy is to assemble *mer*-$[Fe^{III}(qcq)(CN)_3]^-$ anions with $[Mn^{III}$(salen-type)$]^+$ cations. Herein, we report two novel 1-D cyano-bridged bimetallic complexes, $[\{Mn^{III}(salen)\}_2\{Fe^{III}(qcq)(CN)_3\}_2]_n\cdot 3nCH_3CN\cdot nH_2O$ (**1**) and $[\{Mn^{III}(salpn)\}_2\{Fe^{III}(qcq)(CN)_3\}_2]_n\cdot 4nH_2O$ (**2**), based on $[Mn^{III}$(salen-type)$]^+$ and *mer*-$[Fe^{III}(qcq)(CN)_3]^-$ building blocks. For comparison, two 0-D cluster complexes, $[\{Mn^{II}(bipy)(CH_3OH)\}\{Fe^{III}(qcq)(CN)_3\}_2]_2\cdot 2H_2O\cdot 2CH_3OH$ (**3**) and $[\{Mn^{II}(phen)_2\}\{Fe^{III}(qcq)(CN)_3\}_2]\cdot CH_3CN\cdot 2H_2O$ (**4**), derived from $Mn^{II}$ complexes and $[Fe^{III}(qcq)(CN)_3]^-$ have also been synthesized and investigated.

## EXPERIMENTAL SECTION

**Reagents and Materials.** All chemicals and solvents were reagent grade and were used without further purification. $PPh_4[Fe^{III}(qcq)(CN)_3]$,[12f] $[Mn^{III}(salen/salpn)(H_2O)]ClO_4$,[16] $Mn^{II}(bipy)_2Cl_2$, and $Mn^{II}(phen)_2Cl_2$[17] were synthesized according to the methods reported previously.

***Caution!*** *Cyanides are highly toxic and perchlorate salts of metal complexes are potentially explosive. So, handing them carefully with small quantities is highly suggested for safety consideration.*

**Syntheses of Complexes.** *$[\{Mn^{III}(salen)\}_2\{Fe^{III}(qcq)(CN)_3\}_2]_n\cdot 3nCH_3CN\cdot nH_2O$ (**1**).* A methanol solution (10 mL) of $[Mn^{III}(salen)(H_2O)]ClO_4$ (0.05 mmol) was slowly added to an acetonitrile solution (10 mL) of $PPh_4[Fe^{III}(qcq)(CN)_3]$ (0.05 mmol). The resulting solution was filtrated, and the filtrate was left to allow slow evaporation in the dark at room temperature. Black block crystals of complex **1** were formed in two weeks, which were washed with methanol and water, respectively, and dried in air. Yield: 42.1%. Anal. Found: C, 59.52; H, 3.83; N, 16.34; Fe, 6.55; Mn, 6.71%. Calcd for $C_{82}H_{65}Fe_2Mn_2N_{19}O_7$: C, 59.69; H, 3.97; N, 16.63; Fe, 6.76; Mn, 6.66%. IR: $\nu_{max}/cm^{-1}$ 3444(s), 2130(m), 1620(s), 1540(m), 1504(w), 1465(m), 1446(m), 1390(m), 1342(w), 1290(m), 1211(m), 1151(m), 900(w), 769(m).

*$[\{Mn^{III}(salpn)\}_2\{Fe^{III}(qcq)(CN)_3\}_2]_n\cdot 4nH_2O$ (**2**).* By replacing $[Mn^{III}(salen)(H_2O)]ClO_4$ with $[Mn^{III}(salpn)(H_2O)]ClO_4$, complex

**Table 1. Details of the Crystallographic Data Collection, Structural Determination, and Refinement for 1−4**

| | 1 | 2 | 3 | 4 |
|---|---|---|---|---|
| formula | $C_{82}H_{65}Fe_2Mn_2N_{19}O_7$ | $C_{78}H_{64}Fe_2Mn_2N_{16}O_{10}$ | $C_{56}H_{42}Fe_2MnN_{14}O_5$ | $C_{70}H_{47}Fe_2MnN_{17}O_4$ |
| $f_W$ | 1650.11 | 1607.03 | 1157.68 | 1356.89 |
| cryst syst | monoclinic | monoclinic | triclinic | triclinic |
| space group | $P2_1/c$ | $P2_1/c$ | $P\bar{1}$ | $P\bar{1}$ |
| $a$/Å | 17.4103(15) | 17.6439(15) | 13.184(3) | 12.6301(13) |
| $b$/Å | 23.7012(17) | 23.7322(17) | 13.904(3) | 16.0901(15) |
| $c$/Å | 20.3902(11) | 20.535(2) | 15.349(3) | 17.9602(14) |
| $\alpha$/deg | 90.00 | 90.00 | 95.66(3) | 96.881(2) |
| $\beta$/deg | 104.701(2) | 105.385(3) | 106.30(3) | 109.572(3) |
| $\gamma$/deg | 90.00 | 90.00 | 98.89(3) | 109.261(2) |
| $V$/Å$^3$ | 8138.5(10) | 8290.4(13) | 2638.0(9) | 3135.8(5) |
| $Z$ | 4 | 4 | 2 | 2 |
| $\rho_{calcd}$ /g cm$^{-3}$ | 1.347 | 1.288 | 1.457 | 1.437 |
| $F(000)$ | 3392 | 3304 | 1186 | 1390 |
| $\theta$/deg | 3.13−25.33 | 1.2−26.00 | 3.11−26.00 | 3.24−25.36 |
| index ranges | $-20 \le h \le 16$ | $-21 \le h \le 20$ | $-16 \le h \le 16$ | $-15 \le h \le 15$ |
| | $-26 \le k \le 28$ | $-27 \le k \le 29$ | $-17 \le k \le 14$ | $-19 \le k \le 17$ |
| | $-21 \le l \le 24$ | $-24 \le l \le 25$ | $-18 \le l \le 18$ | $-21 \le l \le 20$ |
| total/unique data | 40 849/14 721 | 53 089/16 300 | 20 213/10 047 | 24 399/11 274 |
| obsd data $[I > 2\sigma(I)]$ | 12 029 | 11 635 | 7589 | 8431 |
| $R_{int}$ | 0.0310 | 0.0511 | 0.0502 | 0.0404 |
| data/restraints/params | 12 029/0/1027 | 11 635/0/1029 | 7589/1/727 | 8431/0/867 |
| GOF on $F^2$ | 1.074 | 1.052 | 1.061 | 1.026 |
| R1 $[I > 2\sigma(I)]$ | 0.0475 | 0.0587 | 0.0883 | 0.0585 |
| wR2 (all data) | 0.1246 | 0.1321 | 0.2289 | 0.1171 |


dx.doi.org/10.1021/ic401753y | *Inorg. Chem.* 2014, 53, 116−127

**Scheme 2. Solvent Effect on the Reaction of $[Mn^{III}(salen)(H_2O)]ClO_4$ with $PPh_4[Fe^{III}(qcq)(CN)_3]$**

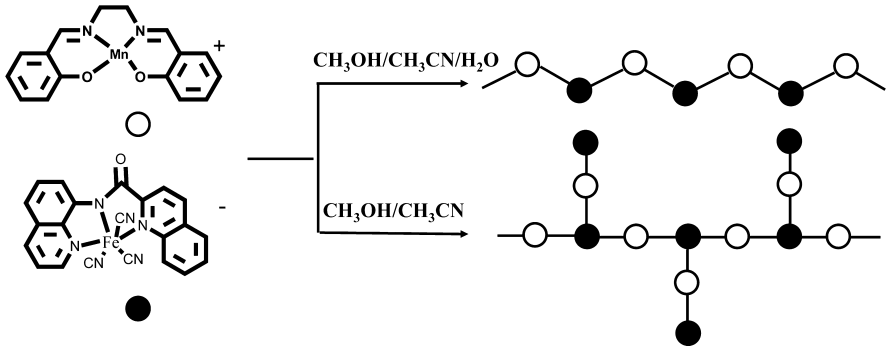


**Table 2. Selected Bond Lengths (Å) and Angles (deg) for 1–4**

| 1 | | 2 | | 3 | | 4 | |
|---|---|---|---|---|---|---|---|
| C1–Fe1 | 1.930(3) | C1–Fe1 | 1.953(3) | C1–Fe1 | 1.946(5) | C1–Fe1 | 1.938(3) |
| C2–Fe1 | 1.962(3) | C2–Fe1 | 1.980(3) | C2–Fe1 | 1.947(7) | C2–Fe1 | 1.955(4) |
| C3–Fe1 | 1.906(3) | C3–Fe1 | 1.928(4) | C3–Fe1 | 1.965(5) | C3–Fe1 | 1.936(3) |
| C4–Fe2 | 1.918(3) | C4–Fe2 | 1.894(4) | C4–Fe2 | 1.968(6) | C4–Fe2 | 1.933(4) |
| C5–Fe2 | 1.965(3) | C5–Fe2 | 2.068(3) | C5–Fe2 | 1.954(6) | C5–Fe2 | 1.920(3) |
| C6–Fe2[a] | 1.921(3) | C6–Fe2 | 2.043(3) | C6–Fe2 | 1.942(6) | C6–Fe2 | 1.978(4) |
| N8–Fe1 | 1.893(2) | N8–Fe1 | 1.880(3) | N8–Fe1 | 1.882(4) | N8–Fe1 | 1.851(3) |
| N7–Fe1 | 1.994(2) | N7–Fe1 | 1.987(2) | N7–Fe1 | 1.999(6) | N9–Fe1 | 1.959(2) |
| N9–Fe1 | 2.017(2) | N9–Fe1 | 2.028(3) | N9–Fe1 | 2.016(6) | N7–Fe1 | 2.010(2) |
| N13–Fe2 | 1.867(2) | N13–Fe2 | 1.906(3) | N11–Fe2 | 1.875(6) | N15–Fe2 | 1.890(3) |
| N14–Fe2 | 1.957(2) | N14–Fe2 | 1.918(3) | N12–Fe2 | 1.932(6) | N16–Fe2 | 1.951(2) |
| N12–Fe2 | 2.131(2) | N12–Fe2 | 2.129(3) | N10–Fe2 | 2.111(6) | N14–Fe2 | 1.951(2) |
| Mn1–N3 | 2.249(2) | Mn1–N3 | 2.242(3) | Mn1–N6[d] | 2.176(5) | Mn1–N3 | 2.166(2) |
| Mn1–N4 | 2.280(6) | Mn1–N4 | 2.253(3) | Mn1–O3 | 2.193(3) | Mn1–N4 | 2.194(3) |
| Mn2–N6 | 2.298(4) | Mn2–N6 | 2.259(2) | Mn1–N1 | 2.222(5) | Mn1–N11 | 2.201(2) |
| Mn2–N5 | 2.319(4) | Mn2–N5 | 2.270(2) | Mn1–N4 | 2.231(5) | Mn1–N13 | 2.213(2) |
| N1–C1–Fe1 | 177.8(2) | N1–C1–Fe1 | 175.0(3) | Mn1–N14 | 2.255(6) | Mn1–N12 | 2.262(2) |
| N2–C2–Fe1 | 179.2(2) | N2–C2–Fe1 | 175.9(3) | Mn1–N13 | 2.258(3) | Mn1–N10 | 2.270(3) |
| N3–C3–Fe1 | 172.7(2) | N3–C3–Fe1 | 173.1(3) | N1–C1–Fe1 | 178.2(5) | N1–C1–Fe1 | 176.7(2) |
| N4–C4–Fe2 | 178.4(2) | N4–C4–Fe2 | 175.9(3) | N2–C2–Fe1 | 177.0(6) | N2–C2–Fe1 | 174.0(3) |
| N5–C5–Fe2 | 173.1(2) | N5–C5–Fe2 | 148.8(3) | N3–C3–Fe1 | 174.9(5) | N3–C3–Fe1 | 178.2(2) |
| N6–C6–Fe2[a] | 174.7(2) | N6[b]–C6-Fe2 | 151.0(3) | N4–C4–Fe2 | 172.6(5) | N4–C4–Fe2 | 177.3(3) |
| C3–N3–Mn1 | 162.8(2) | C3–N3–Mn1 | 168.7(3) | N5–C5–Fe2 | 173.8(5) | N5–C5–Fe2 | 177.5(3) |
| C4–N4–Mn1 | 162.4(2) | C4–N4–Mn1 | 166.6(3) | N6–C6–Fe2 | 174.1(5) | N6–C6–Fe2 | 177.7(3) |
| C5–N5–Mn2 | 157.8(2) | C5–N5–Mn2 | 172.2(3) | C1–N1–Mn1 | 164.3(4) | C3–N3–Mn1 | 176.4(2) |
| C6–N6–Mn2 | 155.9(2) | C6[c]–N6-Mn2 | 172.7(3) | C4–N4–Mn1 | 152.2(4) | C4–N4–Mn1 | 163.6(2) |
| | | | | C6–N6–Mn1[d] | 159.5(4) | | |

[a]Symmetry transformations used to generate equivalent atoms : $x$, $0.5 - y$, $0.5 + z$. [b]Symmetry transformations used to generate equivalent atoms: $x$, $0.5 - y$, $0.5 + z$. [c]Symmetry transformations used to generate equivalent atoms: $x$, $0.5 - y$, $-0.5 + z$. [d]Symmetry transformations used to generate equivalent atoms: $1 - x$, $1 - y$, $1 - z$.

**2** was also obtained as black block crystals according to the same synthetic procedure as complex **1**. Yield: 45.3%. Anal. Found: C, 58.23; H, 4.15; N, 13.69; Fe, 6.81; Mn, 6.93%. Calcd for $C_{78}H_{64}Fe_2Mn_2N_{16}O_{10}$: C, 58.30; H, 4.01; N, 13.95; Fe, 6.75; Mn, 6.84%. IR: $\nu_{max}/cm^{-1}$ 3444(s), 2121(m), 1619(s), 1541(m), 1503(w), 1463(m), 1446(m), 1392(m), 1340(w), 1292(m), 1210(m), 1150(m), 899(w), 767(m).

*$[\{Mn^{II}(bipy)(CH_3OH)\}\{Fe^{III}(qcq)(CN)_3\}_2]_2\cdot 2H_2O\cdot 2CH_3OH$* ***(3)***. Complex **3** was obtained as black block crystals by slow diffusion of a methanol solution (10 mL) of $PPh_4[Fe^{III}(qcq)(CN)_3]$ (0.1 mmol) and an aqueous solution (10 mL) of $Mn^{II}(bipy)_2Cl_2$ (0.05 mmol) through an H-shaped tube at room temperature for about one month. The resulting crystals were collected, washed with $CH_3OH$, and dried in air. Yield: 34.8%. Anal. Found: C, 58.57; H, 3.90; N, 16.38; Fe, 9.41; Mn, 4.49%. Calcd for $C_{56}H_{42}Fe_2MnN_{14}O_5$: C, 58.10; H, 3.65; N, 16.94; Fe, 9.65; Mn, 4.75%. IR: $\nu_{max}/cm^{-1}$ 3446(s), 2121(s), 1635(s), 1504(m), 1465(m), 1441(m), 1388(s), 1342(m), 1214(w), 1153(m), 831 (m), 769(s).

*$[\{Mn^{II}(phen)_2\}\{Fe^{III}(qcq)(CN)_3\}_2]\cdot CH_3CN\cdot 2H_2O$* ***(4)***. An aqueous solution (10 mL) of $Mn^{II}(phen)_2Cl_2$ (0.05 mmol) was slowly added to an acetonitrile solution (10 mL) of $PPh_4[Fe^{III}(qcq)(CN)_3]$ (0.1 mmol). The resulting solution was filtrated, and the filtrate was left to allow slow evaporation in dark at room temperature. Black block crystals of complex **4** were formed in two weeks. The product was washed with methanol and water, respectively, and dried in air. Yield: 64.3%. Anal. Found: C, 61.77; H, 3.65; N, 17.43; Fe, 8.33; Mn, 4.15%. Calcd for $C_{70}H_{47}Fe_2MnN_{17}O_4$: C, 61.96; H, 3.49; N, 17.55; Fe, 8.23; Mn, 4.05%. IR: $\nu_{max}/cm^{-1}$ 3420(s), 3060(m), 2120(s), 1630(s), 1510(m), 1460(m), 1420(m), 1390(s), 1340(m), 1210(m), 1150(m), 850(s), 768(m), 727(m).

**Physical Measurements.** Elemental analyses for C, H, and N were performed at a Perkin-Elmer 240C analyzer. Mn and Fe analyses


dx.doi.org/10.1021/ic401753y | Inorg. Chem. 2014, 53, 116–127

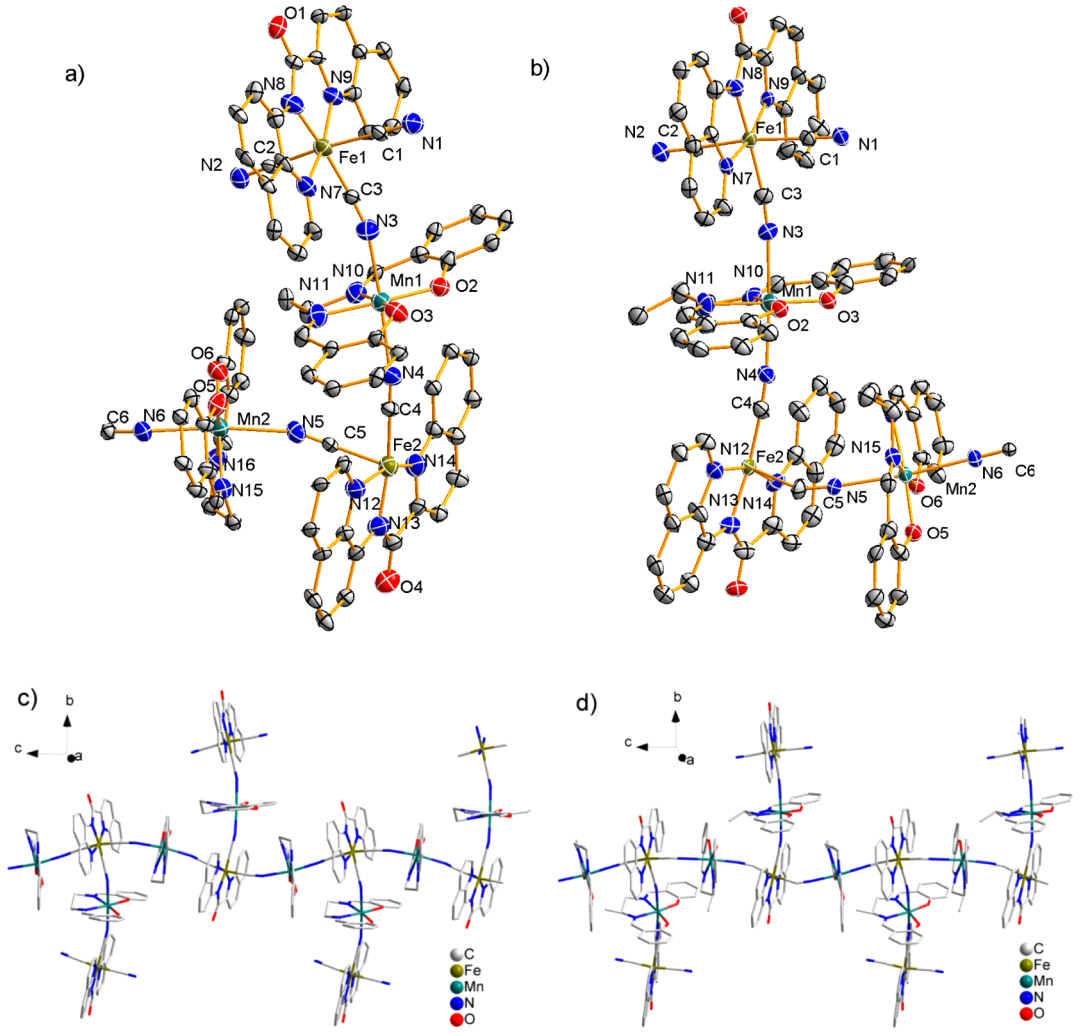


**Figure 1.** ORTEP (30%) diagrams of asymmetric units with selected atom-labeling schemes for **1** (a) and **2** (b), and the 1-D chain structures for **1** (c) and **2** (d) (hydrogen atoms and crystallized solvent molecules are omitted for clarity).

were made on a Jarrell-Ash 1100 + 2000 inductively coupled plasma quantometer (ICP). IR spectra were recorded on a Nicolet FT-170SX spectrometer with KBr pellets in the 4000−400 $cm^{-1}$ region. All magnetic measurements on microcrystalline samples (12.38, 11.29, 9.17, and 10.44 mg for **1**, **2**, **3**, and **4**, respectively) were conducted on a Quantum Design MPMP-XL7 superconducting quantum interference device (SQUID) magnetometer. Corrections of measured susceptibilities were carried out considering both the sample holder as the background and the diamagnetism of the constituent atoms [$-412 \times 10^{-6}$ (**1**, per $Fe^{III}Mn^{III}$), $-401 \times 10^{-6}$ (**2**, per $Fe^{III}Mn^{III}$), $-1158 \times 10^{-6}$ (**3**, per $Fe^{III}_4Mn^{II}_2$), and $-678 \times 10^{-6}$ (**4**, per $Fe^{III}_2Mn^{II}$) $cm^3\ mol^{-1}$] according to Pascal's tables.[18]

**X-ray Structure Determination.** Diffraction data were collected on a Bruker *SMART APEX CCD* area detector diffractometer using graphite-monochromated Mo K$\alpha$ radiation ($\lambda$ = 0.710 73 Å) with the $\varphi$ and $\omega$ scan mode. Diffraction data analysis and reduction were performed with *SMART*, *SAINT*, and *XPREP*.[19] Correction for Lorentz polarization and absorption effects was performed with *SADABS*.[20] Structures were solved using direct method and refined by a full-matrix least-squares techniques based on $F^2$ using *SHELXL-97*.[21] All non-hydrogen atoms were refined with anisotropic thermal parameters. The H atoms of chelated ligands and solvent molecules were calculated at idealized positions and included in the refinement in a riding mode with $U_{iso}$ for H assigned as 1.2 (or 1.5) times $U_{eq}$ of the attached atoms. The water molecules in complex **3** (H-atoms are not found) are disordered, and the oxygen atoms are assigned with partial occupancy of 0.5, 0.35, and 0.15, respectively. The acetonitrile molecules in complex **4** are also disordered in two positions with partial occupancy factor of 0.5 each. The crystallographic data and experimental details for structural analyses are summarized in Table 1. Crystallographic data of complexes **1**, **2**, **3**, and **4** reported in this Article have been deposited at the Cambridge Crystallographic Data Centre as CCDC 944976, 944977, 944978, and 944979, respectively. These data can be obtained free of charge from the Cambridge Crystallographic Data Centre via www.ccdc.cam.ac.uk/data_request/cif.

## RESULTS AND DISCUSSION

**Syntheses and Characterization.** For the reaction of $[Mn^{III}(salen\text{-}type)]^+$ cations with cyanide-containing building blocks, the solvents play a subtle role in determining the self-assembling process of these complexes.[7a] As the reaction of $[Mn^{III}(salen)(H_2O)]ClO_4$ with $PPh_4[Fe^{III}(qcq)(CN)_3]$ is concerned, for instance (Scheme 2), the addition of water into the reaction system affords a 1-D regular zigzag chain complex, $[\{Mn^{III}(salen)\}\{Fe^{III}(qcq)(CN)_3\}]_n \cdot nCH_3CN \cdot nH_2O$ (**1a**).[12f] However, the replacement of water with pure organic solvents (methanol and acetonitrile) in this work results in quite a different structure, which is a unique 1-D linear branch chain with an additional structural unit of $\{Mn^{III}(salen)\}$-$\{Fe^{III}(qcq)(CN)_3\}$ dangling on the two opposite sides of the chain, as revealed by X-ray structure analysis for **1**. Moreover,


dx.doi.org/10.1021/ic401753y | *Inorg. Chem.* 2014, 53, 116−127

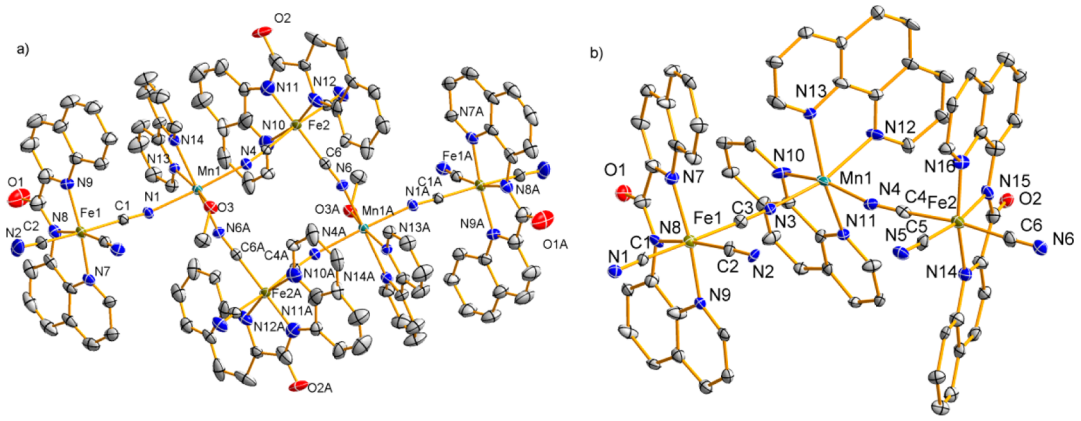


**Figure 2.** ORTEP (30%) diagrams of molecular structures of complexes **3** (a) and **4** (b). (Hydrogen atoms and crystallized solvent molecules are omitted for clarity. Symmetry transformations used to generate equivalent atoms: A = 1 − *x*, 1 − *y*, 1 − *z*.)

with the same reaction conditions, the employment of salpn instead of salen also affords the unique 1-D chain structure similar to **1**, indicating that the solvent effect plays a dominant role in determining the self-assembly mode. For complexes **3** and **4**, the different nuclearity formed can also be ascribed to the different organic solvent used, but the ligand effect can not be neglected because bipy is used for **3** but phen for **4**. IR spectra of **1**−**4** (Figure S1 in Supporting Information) display absorption peaks in the range 2100−2150 $cm^{-1}$, manifesting the presence of cyanide group in these complexes.[13a] The absorption peaks at 1620−1630 and 1400−1600$^{-1}$ $cm^{-1}$ are the stretching vibrations of N═C and benzene ring in the ligands of salen/salpn or qcq. The similarity of the IR spectra of these complexes indicates that they contain the comparable structural units.

**Description of the Structures.** The important structural parameters such as key bond distances and angles are listed in Table 2. The crystal structures of complexes **1**, **2** and **3**, **4** are shown in Figures 1 and 2, respectively. The intermolecular short contacts and $\pi-\pi$ stacking for the four complexes are depicted in Supporting Information Figures S2−S5.

Complexes **1** and **2** are isomorphous though the different Schiff base ligands are used, as demonstrated by the crystal cell parameters listed in Table 1. The asymmetric units of **1** and **2** are composed of two $[Mn^{III}(salen/salpn)]^+$ cations and two $[Fe^{III}(qcq)(CN)_3]^-$ anions, in which one $[Fe^{III}(qcq)(CN)_3]^-$ acts as tridentate ligand to coordinate to three $[Mn^{III}(salen/salpn)]^+$ units with all of its three cyanide groups, and the other one acts as monodentate ligand to coordinate to one $[Mn^{III}(salen/salpn)]^+$ unit, leaving two axial cyanide groups terminal. Each $[Mn^{III}(salen/salpn)]^+$ is *trans*-coordinated by two $[Fe^{III}(qcq)(CN)_3]^-$ through cyanide bridges, forming a 1-D $[-NC-Fe-C\equiv N-Mn-]_n$ linear branch chain with the units of $\{Mn^{III}(salen/salpn)\}\{Fe^{III}(qcq)(CN)_3\}$ dangling on each side of the chain, as shown in Figure 1. To our knowledge, such 1-D branch chain styles for $Mn^{III}$(Schiff-base) based complexes are rarely reported,[5b,6c] and the somewhat comparable chain structures can also be found for Fe−CN−Ni and Cr−CN−Mn series.[5c,9h] For the $[Mn^{III}(salen/salpn)]^+$ cations, salen-type ligands adopt a quasiplanar chelate mode to coordinate to $Mn^{III}$ ion along the equatorial plane, leaving the axial sites coordinated by two N atoms from cyanide groups. The axial $Mn-N_{cyanide}$ bond lengths [2.242(3)−2.319(4) Å] are significantly longer than the equatorial Mn−N/O distances [1.878(2)−2.027(3) Å], affording elongated octahedron configuration derived from Jahn−Teller distortion of $Mn^{III}$. For the bond angle aspect, $\angle Mn-N-C_{cyanide}$ in **1** and **2** [155.9(2)−172.7(3)°] exhibits an obvious deviation from linearity, which is comparable to those in the $[Mn^{III}(Schiff-base)]^+$ based cyano-bridged bimetallic complexes reported before.[15] For the moieties of $[Fe^{III}(qcq)(CN)_3]^-$, the coordination environment of $Fe^{III}$ can also be described as distorted octahedron, consisting of three C atoms from cyanide groups and three N atoms from qcq. The Fe−C(cyanide) bond lengths [1.894(4)−2.043(3) Å ] are overall close to each other, but the Fe−N(qcq) bond distances [1.867(2)-2.131(2) Å] deviate from each other, with the maximum deviations of 0.26 Å for **1** and 0.25 Å for **2**, respectively. The relatively shorter bond distances of Fe−N (amide) [1.867(2)−1.906(3) Å] than Fe−N (aromatic rings) [1.918(3)−2.131(2) Å] could be attributed to the strong $\sigma$-donor effect of the deprotonated amide.[12f] For **1**, the Fe—C≡N angles remain almost linear [172.7(2)−179.2(2)°], comparable to most tricyanidoferrate based bimetallic complexes.[11−14] However for **2**, though the $[Fe^{III}(qcq)(CN)_3]^-$ dangling on sides exhibits almost linear Fe—C≡N angles [173.1(3)−175.9(3)°], the Fe—C≡N angles along the chain direction deviate significantly from linearity with the angles [148.7(3)−151.0(3)°], much smaller than those for **1**, which seem to be somewhat unusual. The shortest intrachain metal−metal distance is 5.221 Å for **1** and 5.218 Å for **2**, respectively. For the extended structures of **1** and **2**, interchain $\pi-\pi$ stacking is observed (Supporting Information Figure S2). The chains stack parallelly each other via the $\pi-\pi$ interaction of the adjacent aromatic ring on $[Fe^{III}(qcq)(CN)_3]^-$, resulting in the formation of 2-D layers. The layers further stack into 3-D supermolecular network via van der Waals interaction (Supporting Information Figure S3). Each of the layers is well separated with the shortest interlayer metal···metal distance of 8.769 Å for **1** and 8.849 Å for **2**, respectively.

In contrast to **1** and **2**, complexes **3** and **4** are cyano-bridged bimetallic hexanuclear and trinuclear clusters, respectively. Though a number of hexanuclear[11b,13b,9b] and trinuclear[13c−f,14a,b] cyano-bridged bimetallic complexes derived from $[Fe^{III}(L)(CN)_3]^-$ and $Mn^{II}$ ions have been investigated, the corresponding assemblies based on *mer*-$[Fe^{III}(qcq)(CN)_3]^-$ building block have not been reported. Complex **3** is made up of neutral centrosymmetric $Fe_4Mn_2$ hexanuclear cluster (Figure 2a), in which two $[Fe^{III}(qcq)(CN)_3]^-$ units each bridge two $Mn^{II}$ ions through cyanide groups in *cis* mode forming a square unit of $[Fe_2Mn_2(CN)_4]^{2+}$, leaving the other two $[Fe^{III}(qcq)-$


dx.doi.org/10.1021/ic401753y | *Inorg. Chem.* 2014, 53, 116−127

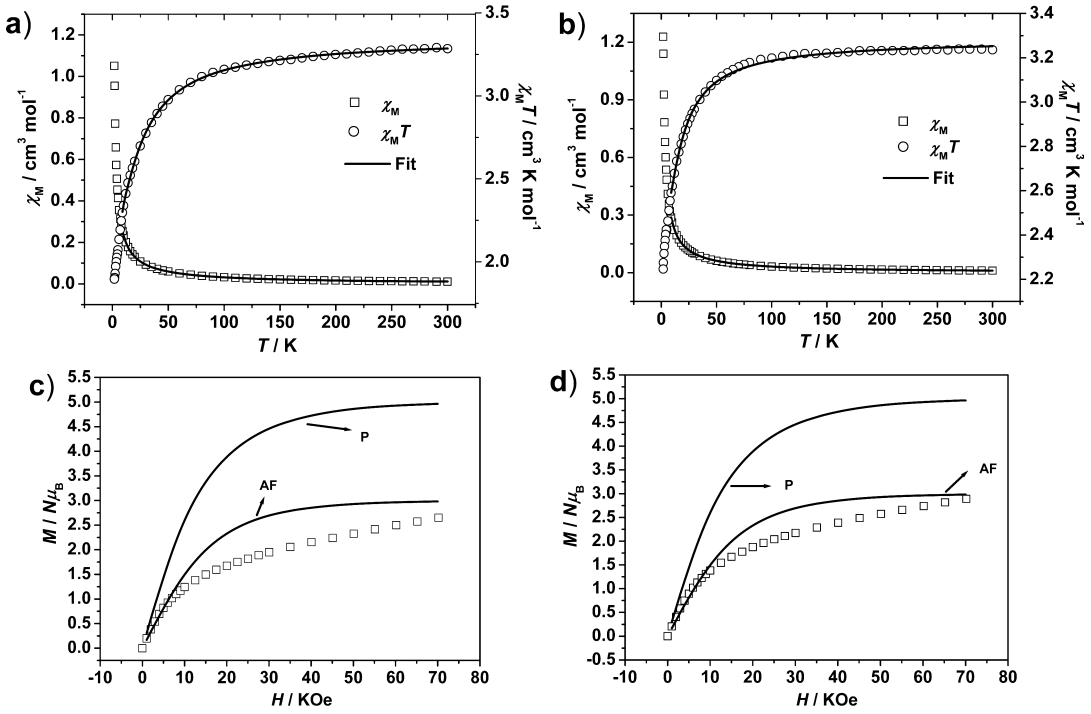


**Figure 3.** Temperature dependence of $\chi_M T$ and $\chi_M$ for **1** (a) and **2** (b) measured at 2 kOe; field dependence of the magnetization for **1** (c) and **2** (d) at 1.8 K. (The curves marked with AF, P represent the theoretical Brillouin curves of antiferromagnetic and paramagnetic states of dimer $Mn^{III}Fe^{III}$ unit, respectively.)

$(CN)_3]^-$ as terminal monodentate ligand binding to the $Mn^{II}$ ions, and resulting in an approximately coplanar hexanuclear entity. The rest of the coordinating sites of each $Mn^{II}$ ion are occupied by one bidentate ligand of bipy and one methanol molecule, forming slightly distorted octahedron geometry around $Mn^{II}$. The $Mn^{II}$–$N_{cyanide}$ bond lengths [2.176(5)–2.231(5) Å] are relatively shorter than the values for $Mn^{II}$–$N_{bipy}$ [2.255(6)–2.258(3) Å]. The angles of Mn–N–$C_{cyanide}$ in **3** are highly bent [152.2(4)–164.3(4)°], which are comparable to the values reported for the analogous complexes.[11b,13b,9b] For the moieties of $[Fe^{III}(qcq)(CN)_3]^-$ in **3**, important structure parameters are comparable to those found for **1**, that is nearly linear Fe—C≡N angles [172.6(5)–178.2(5)°] and highly distorted octahedral coordination configuration around $Fe^{III}$ due to the relatively short Fe–N (amide) bond distances [1.875(6)–1.882(4) Å] as compared with the Fe–N (aromatic ring) ones [1.932(6)–2.111(6) Å]. For the packing mode of **3**, significant intercluster $\pi$–$\pi$ stacking (centroid to centroid distances: 3.768–3.843 Å, Supporting Information Figure S4a) and the abundant hydrogen bonds extend the hexanuclear clusters into 2-D supermolecular layers running parallel to the *ab* plane (Supporting Information Figure S4b). The formed layers are well separated with the shortest interlayer metal–metal distance of 8.964 Å. Different from **3**, complex **4** features V-shaped trinuclear cluster of $Fe_2Mn$ (Figure 2b), where each $[Fe^{III}(qcq)(CN)_3]^-$ unit acts as a monodentate ligand and coordinates to the $Mn^{II}$ ion in *cis*-mode through one of its three cyanide groups. The different nuclearity formed for **3** and **4** should be due to the different coordination environments of the center $Mn^{II}$ ion. As analyzed above, $Mn^{II}$ ions in **3** are only occupied by one bidentate ligand of bipy and one methanol molecule, leaving three coordination sites for $[Fe^{III}(qcq)(CN)_3]^-$ to form the approximately coplanar hexanuclear clusters. However, in the case of **4**, the center $Mn^{II}$ ion is well occupied by two bidentate ligands of phen, leaving only two sites coordinated by two $[Fe^{III}(qcq)(CN)_3]^-$ ions in *cis* mode and generating the V-shaped trinuclear molecular configuration. The main bond parameters of **4** are comparable to those of **3**, but the ∠Mn–N–$C_{cyanide}$ in **4** exhibits a nearly linear structure [176.4(2)°], and is significantly different from that in **3**. In the extended structure of **4**, the clusters first connect each other into a 1-D supermolecular chain via hydrogen bond interactions between the cyano groups and water molecules (Supporting Information Figure S5a), and then interchain $\pi$–$\pi$ stacking (Supporting Information Figure S5b) via aromatic rings from $[Fe^{III}(qcq)(CN)_3]^-$ extends the chains into a 3-D supermolecular hole channel structure (Supporting Information Figure S5c).

**Magnetic Properties.** The temperature dependent magnetic susceptibilities for **1** and **2** were collected at 2 kOe in the temperature range 1.8–300 K (Figure 3a,b). The $\chi_M T$ ($\chi_M$ is the magnetic susceptibility per $Fe^{III}Mn^{III}$ unit) values at 300 K for **1** and **2** are 3.28 and 3.24 cm$^3$ K mol$^{-1}$, respectively, which are close to the spin-only value of 3.38 cm$^3$ K mol$^{-1}$ expected for a magnetically diluted spin system (one $S_{Fe} = {}^1/_2$, one $S_{Mn} = 2$) with $g = 2$. In contrast to dimeric complex $[\{(Tp)Fe^{III}(CN)_3\}\{Mn^{III}(1\text{-napen})(H_2O)\}]\cdot MeCN\cdot 4H_2O$, which exhibits obvious unquenched orbital moment for $Fe^{III}$,[14c] the observed $\chi_M T$ values indicate that spin–orbit coupling of $Fe^{III}$ in **1** and **2** is insignificant. Upon cooling, the $\chi_M T$ values for **1** decrease gradually, but the values for **2** keep nearly constant until 50 K, and then both of them exhibit an abrupt decrease down to 1.89 and 2.25 cm$^3$ K mol$^{-1}$ at 1.8 K, respectively. No maximum was observed in the $\chi_M$ vs $T$ plots. The rapid decrease of $\chi_M T$ in low temperature for **1** and **2** implies the contribution of antiferromagnetic interactions and/or the zero-field splitting (ZFS) effect.[7c,10b,c,12f,14d] From the data, the Curie–Weiss fitting for **1** and **2** based on $\chi_M = C/(T - \theta)$ can


dx.doi.org/10.1021/ic401753y | *Inorg. Chem.* 2014, 53, 116–127

Scheme 3. Schematic Representation of the Fitting Models for (a) 1 and 2 and (b) 3 and 4

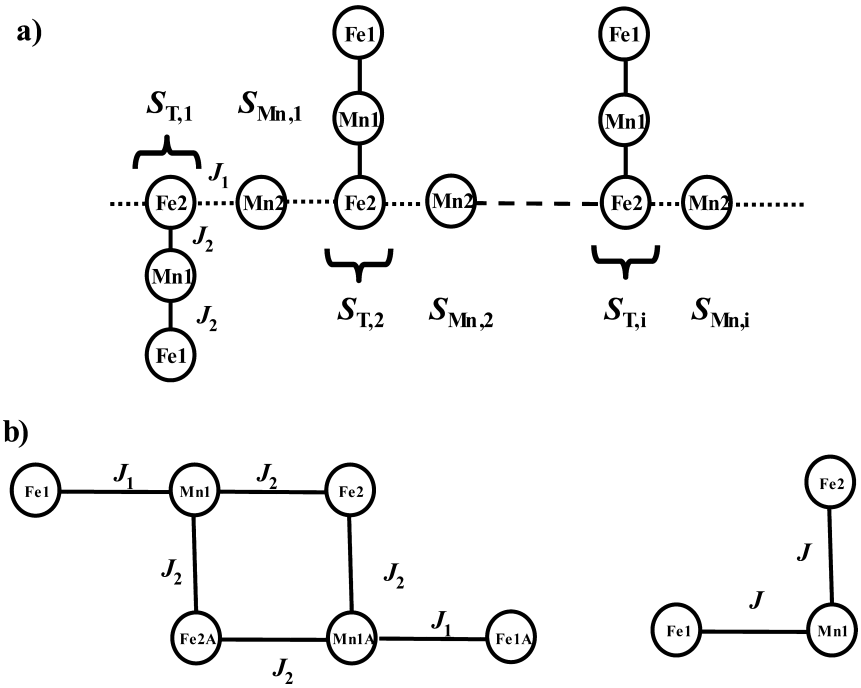


be carried out between 20 and 300 K, affording $C$ = 3.32 cm$^3$ K mol$^{-1}$, $\theta$ = −5.62 K for **1** and $C$ = 3.29 cm$^3$ K mol$^{-1}$, $\theta$ = −3.21 K for **2**, respectively. The negative Weiss constants indicate the possible intramolecular antiferromagnetic interactions for **1** and **2**.

To probe the magnetic exchange coupling between spin carriers, the complicated systems have been first considered as 1-D infinite chain comprising repeating tetranuclear subunits of $Mn^{III}_2Fe^{III}_2$.[7b,d] It is known that this approximate Fisher chain model works only when the intersubunit magnetic interactions are much weaker than the intrasubunit ones. Considering that **1** and **2** show pretty similar Mn−$N_{cyanide}$ bond lengths and Mn−N−$C_{cyanide}$ angles in the chain routes, this model could not describe the present systems. Another approach for evaluating the coupling constant is to use the Magpack[22] program to treat the chains based on a closed ring model.[5c,8b] However, the largest ring the program can calculate contains only two repeating units of the chains. Because the ring model is known to converge to the 1D solution only when about 10 repeating units are considered, this model cannot describe the present systems, either. A third approach considered is the well-known Seiden type model (with quantum $S$ = $^1/_2$ spins and classical $S$ = 2 spins).[23] Unfortunately, there is no available Seiden type analytical expression for such a particular chain, and we have also failed to deduce the rigorous mathematic expression for the susceptibility owing to the particular chain topology. Nevertheless, an approximate approach for treating such type of branch chain reported by S. Gao's group has inspired us to analyze the data of **1** and **2**.[9h] Such approximate treatment has been already widely used for 1-D, 2-D, and quasi-2-D complexes to roughly estimate the $J$ value in previously reported works.[24] From the structural data of **1** and **2**, the Mn−$N_{cyanide}$ bond lengths in the chain routes are longer [**1**, 2.298(4), 2.319(4) Å; **2**, 2.259(2), 2.270(2) Å] than those found in the branches [**1**, 2.249(2), 2.280(6) Å; **2**, 2.242(3), 2.253(3) Å]. Besides, the Mn−N−$C_{cyanide}$ angles in the chain routes [**1**,155.9(2), 157.8(2)°; **2**, 172.2(3), 172.7(3)°] also differ significantly with those in the branches [**1**, 162.4(2), 162.8(2)°; **2**, 166.6(3), 168.7(3)°]. Therefore, **1** and **2** can be considered as uniform chain comprising alternating Fe1−Mn1−Fe2 ($S_T$) trimers (Fe1, Mn1 from the branch) and Mn2 units (Scheme 3a) based on the Hamiltonian (for simplification, zero-field splitting (ZFS) and interchain interation was not considered).

$$H_{chain} = -2J_1 \sum_{-\infty}^{+\infty} (S_{T,i}S_{Mn,i} + S_{T,i+1}S_{Mn,i+1})$$

$$H_{trimer} = -2J_2(S_{Mn1}S_{Fe1} + S_{Mn1}S_{Fe2})$$

The accuracy of this approximate model increases when the Fe···Mn interactions in the chain routes ($J_1$) are actually very weak as compared with $J_2$. The experimental $\chi_M$ values between 10 and 300 K were fitted using the deduced magnetic formula (see Supporting Information), giving $J_1$ = −0.16 cm$^{-1}$, $J_2$ = −2.9 cm$^{-1}$, $g$ = 1.99, $R$ = 3.0 × 10$^{-5}$ for **1** and $J_1$ = −0.32 cm$^{-1}$, $J_2$ = 1.0 cm$^{-1}$, $g$ = 1.97, $R$ = 6.0 × 10$^{-5}$ for **2**, respectively.

The calculated curves for **1** and **2** (solid lines in Figure 3a,b) match very well the magnetic data above 10 K with $J_1$ values indeed much smaller than $J_2$, implying that the complicated 1-D branch chain topology of **1** and **2** can be simplified as 1-D weak coupled Fe1−Mn1−Fe2 ($S_T$) trimers (Fe1, Mn1 from the branch) and the paramagnetic ions of Mn2 units at least from the point of magnetism. The fitting results indicate that all the magnetic pathways in **1** mediate antiferromagnetic interactions while the ferromagnetic and antiferromagnetic interactions might coexist in **2**. The fitting parameters should still be taken with caution since this is the rough model for the complicated systems. However, evidence for the result is then provided by further analysis of the magnetostructural correlation. Field-dependent magnetization measured up to 70 kOe at 1.8 K was performed, as shown in Figure 3c,d. The magnetization of **1** and **2** increases with the increasing external field and reaches 2.65 $N\mu_B$ for **1** and 2.89 $N\mu_B$ for **2** at 70 kOe, respectively, with


dx.doi.org/10.1021/ic401753y | Inorg. Chem. 2014, 53, 116−127

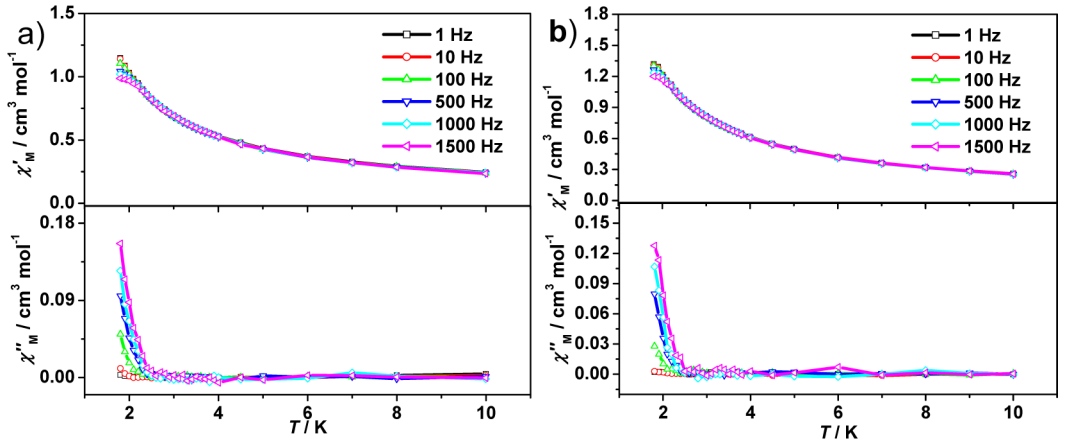


**Figure 4.** Real ($\chi_M'$) and imaginary ($\chi_M''$) parts of ac magnetic susceptibility for **1** (a) and **2** (b) under 0 dc and 3 Oe ac magnetic field.

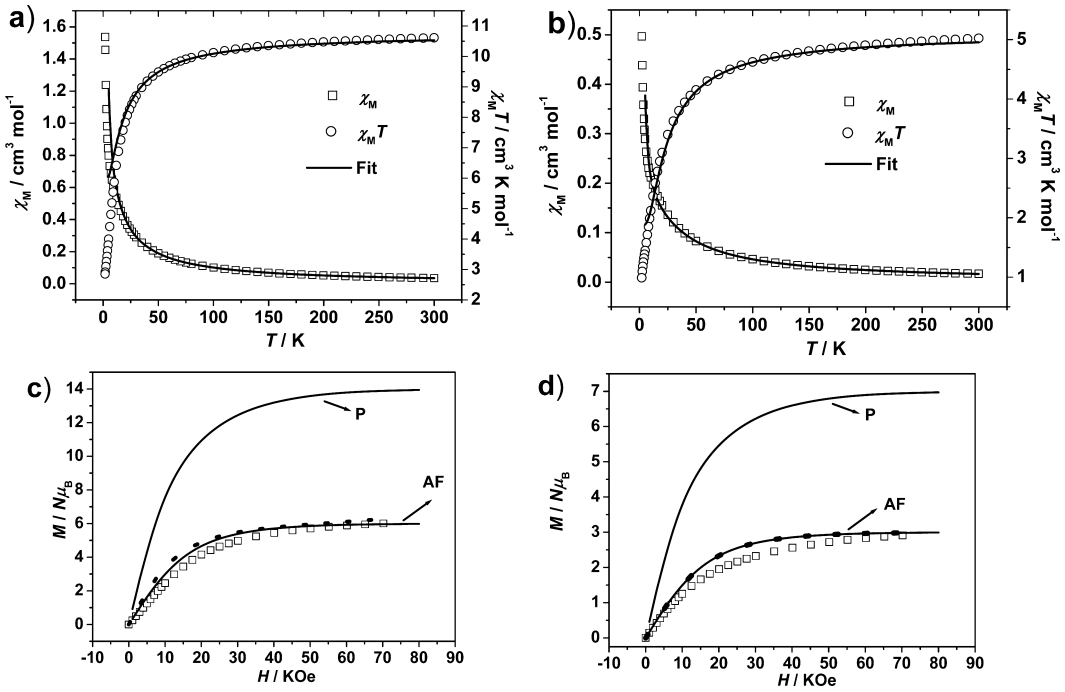


**Figure 5.** Temperature dependence of $\chi_M T$ and $\chi_M$ for **3** (a) and **4** (b) measured at 2 kOe; field dependence of the magnetization for **3** (c) and **4** (d) at 1.8 K. [The curves marked with AF, P represent the theoretical Brillouin curves of antiferromagnetic and paramagnetic states of units of $Fe^{III}_4Mn^{II}_2$ for **3** (c) and $Fe^{III}_2Mn^{II}$ for **4** (d), respectively; the dotted curve represents the theoretical simulated result from the Magpack program.]

the saturation value (3 $N\mu_B$) [calculated from $M_S = g(S_{Mn} - S_{Fe})$ with $g = 2$)] anticipated from antiferromagnetic coupled Mn−NC−Fe unit unattained. For comparison, the theoretical Brillouin curves of antiferromagnetic (AF) and paramagnetic (P) states of $Mn^{III}Fe^{III}$ unit were also plotted in Figure 3c,d. For **1**, the experimental data overall match with AF Brillouin curve, indicating the presence of AF state in **1** at that temperature. The magnetization value for **1** remains unsaturated even at 70 kOe, implying the presence of magnetic anisotropy in such a system.[6c] As the case for **2**, the magnetization at 70 kOe is 2.89 $N\mu_B$, and the obvious upward tendency of the $M-H$ curve indicates that the magnetization is far from saturation and the saturation value should be larger than 3 $N\mu_B$, implying the ferromagnetic contributions might compete with antiferromagnetic ones.

Alternating current (ac) magnetic measurements (Figure 4) reveal that complexes **1** and **2** show detectable frequency dependent $\chi_M'$ and $\chi_M''$ signals in low temperature, indicating the existence of slow magnetic relaxations. The study on the correlation length ($\xi$) of the systems was then performed, as shown by the curves of $\ln(\chi_M'T)$ vs $T^{-1}$ (Supporting Information Figure S6). The curves of $\ln(\chi_M'T)$ decrease as a function of $1/T$ and deviate from linearity, indicating that significant interchain antiferromagnetic interactions occur in low temperature and the 1-D magnetic behaviors are destroyed by the interchain interactions.

The temperature dependence of magnetic susceptibilities for **3** and **4** were also collected at 2 kOe in the temperature range 1.8−300 K (Figure 5a,b). The $\chi_M T$ values at 300 K for **3** (per $Fe^{III}_4Mn^{II}_2$ unit) and **4** (per $Fe^{III}_2Mn^{II}$ unit) are 10.61 and 5.02 $cm^3$ K $mol^{-1}$, respectively, which are close to the spin-only values calculated for $Fe^{III}_4Mn^{II}_2$ unit (10.24 $cm^3$ K $mol^{-1}$) and $Fe^{III}_2Mn^{II}$ unit (5.12 $cm^3$ K $mol^{-1}$) assuming $g_{Fe} = g_{Mn} = 2$. Upon cooling, the $\chi_M T$ values of **3** and **4** both decrease first


dx.doi.org/10.1021/ic401753y | Inorg. Chem. 2014, 53, 116−127

gradually and then rapidly in the low temperature region down to 2.85 $cm^3$ K $mol^{-1}$ for **3** and 0.99 $cm^3$ K $mol^{-1}$ for **4** at 1.8 K. Comparable to **1** and **2**, no maximum was observed in the $\chi_M$ vs $T$ plots of **3** and **4**, indicating there is no antiferromagnetic ordering. The decrease of $\chi_M T$ values implies that the antiferromagnetic interactions dominate in the systems. Curie−Weiss fitting for **3** and **4** in the temperature range 20−300 K affords $C$ = 10.96 $cm^3$ K $mol^{-1}$, $\theta$ = −7.86 K for **3** and $C$ = 5.29 $cm^3$ K $mol^{-1}$, $\theta$ = −13.91 K for **4**, respectively. The negative Weiss constants also indicate the intramolecular antiferromagnetic interactions in **3** and **4**.

To evaluate intramolecular magnetic couplings constants, the hexanuclear and trinuclear cluster models for **3** and **4** were rationally devised, as shown in Scheme 3b. Two interactions ($J_1$, $J_2$) are assigned for **3** and one $J$ for **4** to avoid overparametrization. The Magpack program was employed to treat the data by neglecting the intermolecular interactions and zero-field splitting effect. On the basis of the spin Hamiltonian of **3** [$H = -2J_1(S_{Fe1}S_{Mn1} + S_{Fe1A}S_{Mn1A}) - 2J_2(S_{Fe2}S_{Mn1} + S_{Fe2A}S_{Mn1} + S_{Fe2A}S_{Mn1A} + S_{Fe2}S_{Mn1A})$] and **4** [$H = -2J(S_{Fe1}S_{Mn1} + S_{Fe2}S_{Mn1})$], the best-fit in the temperature range 5−300 K gives $J_1$ = −2.0 $cm^{-1}$, $J_2$ = −1.5 $cm^{-1}$, $g$ = 2.05, $R = 2.1 \times 10^{-4}$ for **3** and $J$ = −4.0 $cm^{-1}$, $g$ = 2.1, $R = 1.2 \times 10^{-4}$ for **4**, respectively.

The fitting results indicate the dominant intramolecular antiferromagnetic interactions in **3** and **4**, which are comparable to the parameters obtained for analogous complexes in the literature.[10d,13c−f,14a,b,e] Field-dependent magnetizations for **3** and **4** were measured from 0 to 70 kOe at 1.8 K (Figure 5c,d). As the applied field increases, the magnetizations continuously increase until reaching 6.01 and 2.91 $N\mu_B$ at 70 kOe for **3** and **4**, respectively. The saturation values are consistent with the theoretical values expected for antiferromagnetic coupled $Fe^{III}_4Mn^{II}_2$ and $Fe^{III}_2Mn^{II}$ units, respectively, which also match well with the theoretical Brillouin and Magpack curves of antiferromagnetic states of $Fe^{III}_4Mn^{II}_2$ and $Fe^{III}_2Mn^{II}$.

Alternating current (ac) magnetic measurements (Supporting Information Figure S7) show no detectable frequency dependent $\chi_M'$ and $\chi_M''$ signals for **3** and **4**, indicating the completely paramagnetic behavior without any magnetic ordering.

**Magnetostructural Correlation.** It is worth noting that the related magnetostructurally characterized analogues based on $Fe^{III}$−$Mn^{III}$ systems,[7c,10b,c,12f,14c,d] were found to be either ferro- or antiferromagnetic coupling. The complicated mechanism for magnetic exchange in the pathway of $Fe^{III}$−CN−$Mn^{III}$ was well analyzed by D. Visinescu et al. through DFT calculations,[10e] which revealed that there are two critical factors in determining the magnetic coupling strength and nature (ferro- or antiferromagnetic). The first factor is molecular orbital describing the unpaired electron in low-spin $Fe^{III}$ center (electronic configuration $t_{2g}^5e_g^0$), and the second one is the angle of Mn−N−$C_{cyanide}$ ($\theta$) involving the cyanide group that connects the $Mn^{III}$ and $Fe^{III}$ centers. The magnetic orbitals on low-spin $Fe^{III}$ in hexacoordinated ligand field can be $d_{xy}$, $d_{yz}$, or $d_{xz}$ type ($z$ axis is defined as the bridging cyanide direction), which are determined by the number and arrangement of the cyanide groups around the iron(III) ion. D. Visinescu et al. found that the tetracyano-bearing iron(III) precursors often prefer a $d_{xy}$ type magnetic orbital, while the *mer*-tricyanidoferrate ones adopt a $d_{xz}$ type instead. For the free cyanide-bearing iron(III), like $[Fe(CN)_6]^{3-}$ or *fac*-tricyanidoferrate, all three $t_{2g}$ orbitals contribute to build the magnetic orbitals. If the unpaired electron is located on the $d_{xy}$ orbital, which does not delocalize any significant spin density on the cyanide bridge, a ferromagnetic coupling independent of bond angles of Mn−N−$C_{cyanide}$ occurs. However, when the $d_{xz}$ type ($d_{yz}$ type is similar to $d_{xz}$ type) orbital is effective due to the structural factors, part of its electron density is delocalized on the $\pi$-pathway of the cyanide ligand, and its interaction with the [($d_{xz}$, $d_{yz}$, $d_{xy}$)$^3$($d_{z^2}$)$^1$] on $Mn^{III}$ leads to one antiferro- ($d_{xz}$−$d_{xz}$) and three ferromagnetic ($d_{xz}$−$d_{xy}$, $d_{xz}$−$d_{yz}$, $d_{xz}$−$d_{z^2}$) contributions (Figure 6). The ferromagnetic contribution from $d_{xz}$−$d_{z^2}$

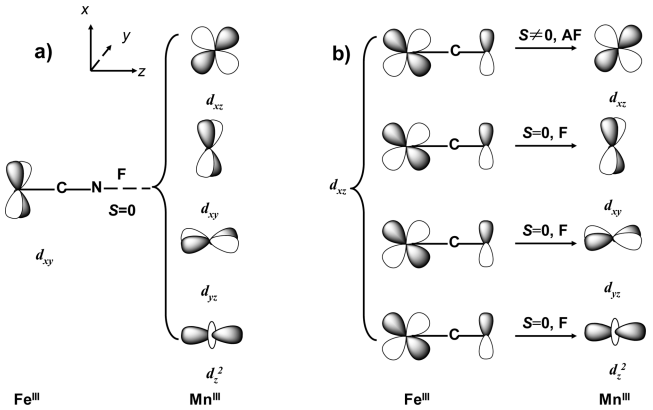


**Figure 6.** Overlap ($S$) between magnetic orbitals of the low-spin $Fe^{III}$ ion and high-spin $Mn^{III}$ through cyanide bridge: (a) magnetic orbital defined as $d_{xy}$ orbital; (b) magnetic orbital defined as $d_{xz}$ orbital.

dominates the other ones, but its orthogonality can be lost as the bending of the Mn−N−$C_{cyanide}$ increases, leading to magnetic coupling type from ferro- to antiferromagnetic. The systems of $Fe^{III}$−$Mn^{II}$ are different from $Fe^{III}$−$Mn^{III}$ because of the contribution from the magnetic orbit of $d_{x^2-y^2}$. The bending of the Mn−N−$C_{cyanide}$ would cause the orbit overlapping between $d_{x^2-y^2}$ and the delocalized electron density on the $\pi$-pathway of the cyanide from $d_{xz}$. Thus, the weak ferromagnetic contributions in $Fe^{III}$−$Mn^{II}$ systems are always overwhelmed by the antiferromagnetic ones, affording the dominant antiferromagnetic interactions. Therefore, the experimental facts (Table 3) that some $Fe^{III}$−$Mn^{III}$ systems exhibit ferromagnetic nature while the others reverse from ferro- to antiferromagnetic when the Mn−N−$C_{cyanide}$ angles are smaller than 165° can be then understood. For magnetic assembling on the basis of $Fe^{III}$−$Mn^{II}$, antiferromagnetic interactions are always observed, as shown in Table 4, which is in accordance with the theoretical analysis.

On the basis of the above analyses, the magnetic behaviors of **1**, **3**, and **4** are understandable, but **2** seems to be somewhat unusual. Let us focus on the magnetic properties of **2**. Generally, the magnetic interactions should be determined by bond parameters such as bond lengths, bond angles, and bond torsion angles. The bond lengths between spin carriers in **1** and **2** are pretty similar, and thus, the critical factors should be the angles. Because the unpaired electron on low-spin $Fe^{III}$ of *mer*-$[Fe^{III}(qcq)(CN)_3]^-$ is defined by the $d_{xz}$ type orbital, the critical angles of Mn−N−$C_{cyanide}$ in **1** [157.8(2)−162.8°(2), smaller than 165°] and **2** [166.6(3)−172.7(3)°, larger than 165°] indicate that they may prefer antiferro- and ferromagnetic couplings, respectively. The magnetic behavior of **1** is consistent with the theoretical prediction while that of **2** shows some inconsistency. The experimental facts reveal that ferro- and antiferromagnetic contributions coexist in **2**. In order


dx.doi.org/10.1021/ic401753y | *Inorg. Chem.* 2014, 53, 116−127

Table 3. Structural and Magnetic Parameters for Related Cyano-Bridged $Fe^{III}$–$Mn^{III}$ Complexes[a]

| complexes | $d_{Mn-N}$/Å | Fe–C–N (deg) | Mn–N–C (deg) | $J_{exp}$/$cm^{-1}$ | ref |
|---|---|---|---|---|---|
| Magnetic Orbital $d_{xy}$ | | | | | |
| $[Mn(3\text{-}MeOsalen)(H_2O)(\mu\text{-}CN)Fe(bpym)(CN)_3]\cdot 4H_2O$ | 2.328 | 173.9 | 156.9 | 1.48 | 10e |
| $[Mn(4\text{-}MeOsalen)(H_2O)(\mu\text{-}CN)Fe(bpym)(CN)_3]\cdot 2H_2O$ | 2.328 | 173.4 | 156.6 | 1.94 | 10e |
| Magnetic Orbital $d_{xz}$ | | | | | |
| **1** | 2.249–2.319 | 172.7–179.2 | 157.8–162.8 | −0.16∼−2.9 | this work |
| **2** | 2.242–2.270 | 148.7–175.8 | 166.6–172.7 | −0.32–1.0 | this work |
| $[\{Fe(qcq)(CN)_3\}\{Mn(3\text{-}MeOsalen)(H_2O)\}]\cdot 2H_2O$ | 2.289,2.287 | 174.2–175.9 | 144.6, 151.3 | −4.7 | 12f |
| $[\{Fe(qcq)(CN)_3\}\{Mn(5\text{-}Clsalen)\}]\cdot 3H_2O$ | 2.280, 2.285 | 174.6–176.2 | 147.7, 161.4 | −5.3 | 12f |
| $[\{Fe(qcq)(CN)_3\}\{Mn(5\text{-}Brsalen)\}]\cdot 2MeOH$ | 2.283, 2.291 | 175.0–176.3 | 147.7, 159.9 | −5.9 | 12f |
| $[\{Fe(qcq)(CN)_3\}\{Mn(salen)\}]\cdot MeCN\cdot H_2O$ | 2.297, 2.298 | 174.1–175.8 | 149.3, 153.5 | −7.1 | 12f |
| $[\{Fe(mpzcq)(CN)_3\}\{Mn(salen)(H_2O)\}]\cdot H_2O$ | 2.275 | 172.6 | 164.2 | −8.6 | 12e |
| $[\{Fe(iqc)(CN)_3\}\{Mn(5\text{-}salen)\}]\cdot p MeOH\cdot q MeCN\cdot r H_2O$ | 2.273–2.315 | 176.5–176.8 | 167.1–174.1 | 3.74 | 10b |
| $[Mn(saltn)(MeOH)Fe(bpClb)(CN)_2]\cdot 3H_2O$ | 2.256 | 171.9 | 167.4 | 3.2 | 10c |
| $[Mn(saltn)(H_2O)Fe(bpmb)(CN)_2]\cdot H_2O$ | 2.272 | 172.5 | 166.7 | 2.1 | 10c |
| $[Mn(saltn)(MeOH)Fe(bpClb)(CN)_2]\cdot 2H_2O$ | 2.268 | 173.1 | 166.6 | 1.6 | 10c |

[a]Abbreviations used for the ligands: Lb = *cis-N,N′*-(2-hydroxybenzylidene)-1,2,2-trimethylcyclopenta-1,3-diamine; 1-napen = *N,N′*-ethylenebis(2-hydroxy-1-naphthylideneiminato) dianion; $bpClb^{2-}$ = Cl-substituted-1,2-bis(pyridine 2-carboxamido)benzenate; $bpmb^{-}$ = $CH_3$-substituted-1,2-bis(pyridine-2-carboxamido)benzenate.

Table 4. Structural and Magnetic Parameters for Related Cyano-Bridged $Fe^{III}$–$Mn^{II}$ Complexes[a]

| complexes | $d_{Mn-N}$/Å | Mn–N–C (deg) | $J_{exp}$/$cm^{-1}$ | ref |
|---|---|---|---|---|
| $[\{Fe\{HB(pz)_3\}(CN)_3\}_2Mn(MeOH)_4]\cdot 2MeOH$ | 2.179 | 167.3 | −7.6 | 14a |
| $[\{Fe(pcq)(CN)_3\}_2\{Mn(phen)_2\}]\cdot CH_3OH\cdot 2H_2O$ | 2.174 | 173.0–149.1 | −4.03 | 13d |
| $[\{Fe(pcq)(CN)_3\}_2\{Mn(bipy)_2\}]\cdot CH_3OH\cdot 2H_2O$ | 2.194 | 172.5–154.1 | −3.73 | 13d |
| $[(bpca)_2Fe_2(CN)_6Mn(CH_3OH)_2(H_2O)_2]\cdot 2H_2O$ | 2.188–2.203 | 170.9, 168.3, 161.8 | −3.28 | 14b |
| $[(Tp)_2Fe_2(CN)_6Mn(CH_3OH)_4]\cdot 2CH_3OH$ | 2.174 | 167.2 | −2.19 | 13f |
| $[\{Mn(DMF)_2(MeOH)_2\}\{Fe(bpb)(CN)_2\}_2]\cdot 2DMF$ | 2.196 | 164.2–167.5 | −1.59 | 10d |
| $[(Tp)_2Fe_2(CN)_6Mn(C_2H_5OH)_4]\cdot 2C_2H_5OH$ | 2.199 | 170 | −1.37 | 14e |
| **3** | 2.176–2.231 | 152.2–164.3 | −2.0∼−1.5 | this work |
| **4** | 2.166, 2.194 | 163.6, 176.4 | −4.0 | this work |
| $[\{Fe(salen)(CN)_2\}_2\{Mn(bipy)_2\}]\cdot CH_3OH\cdot 2H_2O$ | 2.173 | 164.3 | −1.34 | 13c |
| $[\{Mn(MeOH)_4\}\{Fe(bpdmb)(CN)_2\}_2]\cdot 2MeOH\cdot 2H_2O$ | 2.145 | 164.2–167.5 | −1.32 | 10d |
| $[\{Fe(salen)(CN)_2\}_2\{Mn(phen)_2\}]\cdot CH_3OH$ | 2.172 | 159.9 | −1.23 | 13c |
| $[\{Fe(pcq)(CN)_3\}_2\{Mn(CH_3OH)_2(H_2O)_2\}]\cdot 2H_2O$ | 2.195 | 171.1 | −1.11 | 13d |
| $[\{Fe(bipy)(CN)_4\}_2Mn(H_2O)_4]\cdot 4H_2O$ | 2.183 | 159.5 | −0.45 | 13e |

[a]Abbreviations used for the ligands: $HB(pz)_3$ = hydrotris(1-pyrazolyl)borate; $pcq^{-}$ = 8-(pyridine-2-carboxamido)quinoline anion; $bpca^{-}$ = bis(2-pyridylcarbonyl)amidate; $bpb^{2-}$ = 1,2-bis(pyridine-2-carboxamido)benzenate; $bpdmb^{2-}$ = 1,2-bis(pyridine-2-carboxamido)-4, 5-dimethyl-benzenate.

to understand the unconventional behavior of **2**, we re-examined the structure of **2** and found that the Fe—C≡N angles at the primary chain deviate significantly from linearity with the values [148.7(3)–151.0(3)°] much smaller than those found for the dangling moieties [173.1(3)–175.9(3)°]. Moreover, the corresponding Mn–NC–Fe torsion angles for the primary chain are also much smaller (9.0, 10.1°) than those found for the dangling moieties (30.9, 81.9°). The unusual bent Fe—C≡N angles and the small torsion angles of **2** might be responsible for the decrease of the orbital orthogonality, leading to an antiferromagnetic Mn–NC–Fe pathway ($J_1$) for the primary chain but a ferromagnetic one ($J_2$) for the branch. It is worth noting that, in previous reports, the Fe—C≡N angles always exhibit nearly linear structure with few exceptions, and thus less attention has been paid to them in the analysis of magnetostructural correlation. Consequently, the full understanding of this magnetic behavior induced by unusual Fe–C≡N angles deserves further investigation.

## CONCLUSION

In summary, four heterobimetallic cyano-bridged $Mn^{III/II}$ based complexes **1**–**4** constructed from *mer*-$[Fe^{III}(qcq)(CN)_3]^{-}$ have been synthesized and characterized. It is found the solvent effect plays an important role in determining the structural styles of these complexes. The structural analysis reveals that **1** and **2** feature a novel 1-D linear chain structure with additional structural units alternately dangling on the two sides, while **3** and **4** are cyano-bridged bimetallic hexanuclear and trinuclear clusters, respectively. Further magnetic studies show that dominant intramolecular antiferromagnetic couplings are presented in **1**, **3**, and **4**, while ferromagnetic and antiferromagnetic interactions coexist in **2**. Associated with the theoretical analysis result, complexes **1**–**4** provide further valuable experimental evidence to fully understand the complicated magnetostructural correlation of the fascinating $Fe^{III}$–CN–$Mn^{III/II}$ systems. Moreover, ac frequency dependent $\chi_M'$ and $\chi_M''$ signals for **1** and **2** again reflect the importance of introducing anisotropic $Mn^{III}$ ions in the design of new low-dimensional magnets.


dx.doi.org/10.1021/ic401753y | Inorg. Chem. 2014, 53, 116–127

## ■ ASSOCIATED CONTENT

### Supporting Information

X-ray crystallographic data for complexes **1**−**4** in CIF format, the IR spectroscopy and the intermolecular short contacts and packing diagrams of **1**−**4** in Figures S1−S5, and the additional magnetic diagrams in Figures S6−S7. This material is available free of charge via the Internet at http://pubs.acs.org.

## ■ AUTHOR INFORMATION


### Corresponding Author

*E-mail: xiaopingshen@163.com. Phone: +86-511-88791800. Fax: +86-511-88791800.


### Notes

The authors declare no competing financial interest.

## ■ ACKNOWLEDGMENTS


The authors are grateful for financial support from the National Natural Science Foundation of China (Nos. 51072071, 51272094 and 1601310042) and Doctoral Innovation Program Foundation of China (1721310119).


## ■ REFERENCES


(1) (a) Sessoli, R.; Gatteschi, D.; Caneschi, A.; Novak, M. A. *Nature* **1993**, *365*, 141. (b) Hill, S.; Edwards, R. S.; Aliaga-Alcalde, N.; Christou, G. *Science* **2003**, *302*, 1015. (c) Roch, N.; Florens, S.; Bouchiat, V.; Wernsdorfer, W.; Balestro, F. *Nature* **2008**, *453*, 633. (d) Timco, G. A.; Carretta, S.; Troiani, F.; Tuna, F.; Pritchard, R. G.; McInnes, E. J. L.; Ghirri, A.; Candini, A.; Santini, P.; Amoretti, G.; Affronte, M.; Winpenny, R. E. P. *Nat. Nanotechnol.* **2009**, *4*, 173. (e) Sun, H. L.; Wang, Z. M.; Gao, S. *Coord. Chem. Rev.* **2010**, *254*, 1081. (f) Troiani, F.; Affronte, M. *Chem. Soc. Rev.* **2011**, *40*, 3119. (g) Clemente-Juan, J. M.; Coronado, E.; Gaita-Ariño, A. *Chem. Soc. Rev.* **2012**, *41*, 7464.

(2) (a) Caneschi, A.; Gatteschi, D.; Sessoli, R.; Barra, A. L.; Brunel, L. C.; Guillot, M. *J. Am. Chem. Soc.* **1991**, *113*, 5873. (b) Murugesu, M.; Habrych, M.; Wernsdorfer, W.; Abboud, K. A.; Christou, G. *J. Am. Chem. Soc.* **2004**, *126*, 4766. (c) Ako, A. M.; Hewitt, I. J.; Mereacre, V.; Clerac, R.; Wernsdorfer, W.; Anson, C. E.; Powell, A. K. *Angew. Chem., Int. Ed.* **2006**, *45*, 4926. (d) Lin, P. H.; Burchell, T. J.; Ungur, L.; Chibotaru, L. F.; Wernsdorfer, W.; Murugesu, M. *Angew. Chem., Int. Ed.* **2009**, *48*, 9489. (e) Papatriantafyllopoulou, C.; Wernsdorfer, W.; Abboud, K.; Christou, G. *Inorg. Chem.* **2011**, *50*, 421. (f) Holynska, M.; Premuzic, D.; Jeon, I. R.; Wernsdorfer, W.; Clerac, R.; Dehnen, S. *Chem.—Eur. J.* **2011**, *17*, 9605. (g) Nakano, M.; Oshio, H. *Chem. Soc. Rev.* **2011**, *40*, 3239. (h) Tsai, H. L.; Yang, C. I.; Wernsdorfer, W.; Huang, S. H.; Jhan, S. Y.; Liu, M. H.; Lee, G. H. *Inorg. Chem.* **2012**, *51*, 13171.

(3) (a) Caneschi, A.; Gatteschi, D.; Lalioti, N.; Sangregorio, C.; Sessoli, R.; Venturi, G.; Vindigni, A.; Rettori, A.; Pini, M. G.; Novak, M. A. *Angew. Chem., Int. Ed.* **2001**, *40*, 1760. (b) Clerac, R.; Miyasaka, H.; Yamashita, M.; Coulon, C. *J. Am. Chem. Soc.* **2002**, *124*, 12837. (c) Lescouëzec, R.; Vaissermann, J.; Ruiz-Pérez, C.; Lloret, F.; Carrasco, R.; Julve, M.; Verdaguer, M.; Dromzee, Y.; Gatteschi, D.; Wernsdorfer, W. *Angew. Chem., Int. Ed.* **2003**, *42*, 1483. (d) Chakov, N. E.; Wernsdorfer, W.; Abboud, K. A.; Christou, G. *Inorg. Chem.* **2004**, *43*, 5919. (e) Lescouëzec, R.; Toma, L. M.; Vaissermann, J.; Verdaguer, M.; Delgado, F. S.; Ruiz-Pérez, C.; Lloret, F.; Julve, M. *Coord. Chem. Rev.* **2005**, *249*, 2691.

(4) (a) Bernot, K.; Bogani, L.; Caneschi, A.; Gatteschi, D.; Sessoli, R. *J. Am. Chem. Soc.* **2006**, *128*, 7947. (b) Miyasaka, H.; Madanbashi, T.; Sugimoto, K.; Nakazawa, Y.; Wernsdorfer, W.; Sugiura, K.-I.; Yamashita, M.; Coulon, C.; Clerac, R. *Chem.—Eur. J.* **2006**, *12*, 7028. (c) Visinescu, D.; Madalan, A. M.; Andruh, M.; Duhayon, C.; Sutter, J. P.; Ungur, L.; Van den Heuvel, W.; Chibotaru, L. F. *Chem.—Eur. J.* **2009**, *15*, 11808. (d) Liu, T.; Zhang, Y.-J.; Kanegawa, S.; Sato, O. *J. Am. Chem. Soc.* **2010**, *132*, 8250. (e) Harris, T. D.; Bennett, M. V.; Clerac, R.; Long, J. R. *J. Am. Chem. Soc.* **2010**, *132*, 3980. (f) Boeckmann, J.; Nather, C. *Chem. Commun.* **2011**, *47*, 7104. (g) Dong, D. P.; Liu, T.; Kanegawa, S.; Kang, S.; Sato, O.; He, C.; Duan, C. Y. *Angew. Chem., Int. Ed.* **2012**, *51*, 5119. (h) Feng, X. W.; Liu, J. J.; Harris, T. D.; Hill, S.; Long, J. R. *J. Am. Chem. Soc.* **2012**, *134*, 7521. (i) Dunbar, K. R. *Inorg. Chem.* **2012**, *51*, 12055.

(5) (a) Song, Y.; Zhang, P.; Ren, X. M.; Shen, X. F.; Li, Y. Z.; You, X. Z. *J. Am. Chem. Soc.* **2005**, *127*, 3708. (b) Ni, Z.-H.; Zheng, L.; Zhang, L.-F.; Cui, A.-L.; Ni, W.-W.; Zhao, C.-C.; Kou, H.-Z. *Eur. J. Inorg. Chem.* **2007**, 1240. (c) Costa, V.; Lescouezec, R.; Vaissermann, J.; Herson, P.; Journaux, Y.; Araujo, M. H.; Clemente-Juan, J. M.; Lloret, F.; Julve, M. *Inorg. Chim. Acta* **2008**, *361*, 3912. (d) Freedman, D. E.; Jenkins, D. M.; Long, J. R. *Chem. Commun.* **2009**, 4829. (e) Bernhardt, P. V.; Martinez, M.; Rodriguez, C. *Inorg. Chem.* **2009**, *48*, 4787. (f) Zhu, X.; Zhao, J. W.; Li, B. L.; Song, Y.; Zhang, Y. M.; Zhang, Y. *Inorg. Chem.* **2010**, *49*, 1266.

(6) (a) Zhang, Y. Z.; Wang, B. W.; Sato, O.; Gao, S. *Chem. Commun.* **2010**, *46*, 6959. (b) Svendsen, H.; Jorgensen, M. R.; Overgaard, J.; Chen, Y. S.; Chastanet, G.; Letard, J. F.; Kato, K.; Takata, M.; Iversen, B. B. *Inorg. Chem.* **2011**, *50*, 10974. (c) Zhou, H.-B.; Zhang, Z.-C.; Chen, Y.; Song, Y.; You, X.-Z. *Polyhedron* **2011**, *30*, 3158. (d) Miyasaka, H.; Madanbashi, T.; Saitoh, A.; Motokawa, N.; Ishikawa, R.; Yamashita, M.; Bahr, S.; Wernsdorfer, W.; Clerac, R. *Chem.—Eur. J.* **2012**, *18*, 3942. (e) Guo, Y.; Xu, G. F.; Wang, C.; Cao, T. T.; Tang, J.; Liu, Z. Q.; Ma, Y.; Yan, S. P.; Cheng, P.; Liao, D. Z. *Dalton Trans.* **2012**, *41*, 1624. (f) Chorazy, S.; Nakabayashi, K.; Imoto, K.; Mlynarski, J.; Sieklucka, B.; Ohkoshi, S. *J. Am. Chem. Soc.* **2012**, *134*, 16151.

(7) (a) Zhou, H. B.; Wang, J.; Wang, H. S.; Xu, Y. L.; Song, X. J.; Song, Y.; You, X. Z. *Inorg. Chem.* **2011**, *50*, 6868. (b) Kou, H.-Z.; Zhou, B. C.; Liao, D.-Z.; Wang, R.-J.; Li, Y. *Inorg. Chem.* **2002**, *41*, 6887. (c) Miyasaka, H.; Ieda, H.; Matsumoto, N.; Re, N.; Crescenzi, R.; Floriani, C. *Inorg. Chem.* **1998**, *37*, 255. (d) Yoo, H. S.; Ko, H. H.; Ryu, D. W.; Lee, J. W.; Yoon, J. H.; Lee, W. R.; Kim, H. C.; Koh, E. K.; Hong, C. S. *Inorg. Chem.* **2009**, *48*, 5617.

(8) (a) Ni, Z. H.; Kou, H. Z.; Zhang, L. F.; Ge, C.; Cui, A. L.; Wang, R. J.; Li, Y.; Sato, O. *Angew. Chem., Int. Ed.* **2005**, *44*, 7742. (b) Kou, H. Z.; Ni, Z. H.; Liu, C. M.; Zhang, D. Q.; Cui, A. Li. *New J. Chem.* **2009**, *33*, 2296. (c) Boldog, I.; Munoz-Lara, F. J.; Gaspar, A. B.; Munoz, M. C.; Seredyuk, M.; Real, J. A. *Inorg, Chem.* **2009**, *48*, 3710. (d) Liu, T.; Zhang, Y. J.; Kanegawa, S.; Sato, O. *Angew. Chem., Int. Ed.* **2010**, *49*, 8645. (e) Yao, M. X.; Wei, Z. Y.; Gu, Z. G.; Zheng, Q.; Xu, Y.; Zuo, J. L. *Inorg. Chem.* **2011**, *50*, 8636. (f) Zhang, Y. Z.; Mallik, U. P.; Clerac, R.; Rath, N. P.; Holmes, S. M. *Chem. Commun.* **2011**, *47*, 7194. (g) Yao, M. X.; Zheng, Q.; Cai, X. M.; Li, Y. Z.; Song, Y.; Zuo, J. L. *Inorg. Chem.* **2012**, *51*, 2140.

(9) (a) Lescouezec, R.; Vaissermann, J.; Lloret, F.; Julve, M.; Verdaguer, M. *Inorg. Chem.* **2002**, *41*, 5943. (b) Kim, J.; Han, S.; Pokhodnya, K. I.; Migliori, J. M.; Miller, J. S. *Inorg. Chem.* **2005**, *44*, 6983. (c) Li, D.; Parkin, S.; Clerac, R.; Holmes, S. M. *Inorg. Chem.* **2006**, *45*, 7569. (d) Gu, Z. G.; Yang, Q. F.; Liu, W.; Song, Y.; Li, Y. Z.; Zuo, J. L.; You, X. Z. *Inorg. Chem.* **2006**, *45*, 8895. (e) Shatruk, M.; Dragulescu-Andrasi, A.; Chambers, K. E.; Stoian, S. A.; Bominaar, E. L.; Achim, C.; Dunbar, K. R. *J. Am. Chem. Soc.* **2007**, *129*, 6104. (f) Pan, F.; Wang, Z. M.; Gao, S. *Inorg. Chem.* **2007**, *46*, 10221. (g) Freiherr von Richthofen, C. G.; Stammler, A.; Bogge, H.; DeGroot, M. W.; Long, J. R.; Glaser, T. *Inorg. Chem.* **2009**, *48*, 10165. (h) Zhang, Y. Z.; Gao, S.; Wang, Z. M.; Su, G.; Sun, H. L.; Pan, F. *Inorg. Chem.* **2005**, *44*, 4534.

(10) (a) Nastase, S.; Maxim, C.; Andruh, M.; Cano, J.; Ruiz-Perez, C.; Faus, J.; Lloret, F.; Julve, M. *Dalton Trans.* **2011**, *40*, 4898. (b) Yoo, I. Y.; Ryu, D. W.; Yoon, J. H.; Sohn, A. R.; Lim, K. S.; Cho, B. K.; Koh, E. K.; Hong, C. S. *Dalton Trans.* **2012**, *41*, 1776. (c) Ni, Z. H.; Tao, J.; Wernsdorfer, W.; Cui, A. L.; Kou, H. Z. *Dalton Trans.* **2009**, 2788. (d) Zhang, D. P.; Zhang, L. F.; Chen, X.; Ni, Z. H. *Transition Met. Chem.* **2011**, *36*, 539. (e) Visinescu, D.; Toma, L. M.; Cano, J.; Fabelo, O.; Ruiz-Perez, C.; Labrador, A.; Lloret, F.; Julve, M. *Dalton Trans.* **2010**, *39*, 5028.

(11) (a) Li, D.; Parkin, S.; Wang, G.; Yee, G. T.; Clerac, R.; Wernsdorfer, W.; Holmes, S. M. *J. Am. Chem. Soc.* **2006**, *128*, 4214. (b) Gheorghe, R.; Kalisz, M.; Clerac, R.; Mathoniere, C.; Herson, P.; Li, Y.; Seuleiman, M.; Lescouezec, R.; Lloret, F.; Julve, M. *Inorg. Chem.* **2010**, *49*, 11045. (c) Peng, Y. H.; Meng, Y. F.; Hu, L.; Li, Q. X.; Li, Y. Z.; Zuo, J. L.; You, X. Z. *Inorg. Chem.* **2010**, *49*, 1905. (d) Mercurol, J.; Li, Y.; Pardo, E.; Risset, O.; Seuleiman, M.; Rousseliere, H.; Lescouezec, R.; Julve, M. *Chem. Commun.* **2010**, *46*, 8995. (e) Nihei, M.; Sekine, Y.; Suganami, N.; Nakazawa, K.; Nakao, A.; Nakao, H.; Murakami, Y.; Oshio, H. *J. Am. Chem. Soc.* **2011**, *133*, 3592. (f) Li, D.; Parkin, S.; Wang, G.; Yee, G. T.; Holmes, S. M. *Inorg. Chem.* **2006**, *45*, 1951. (g) Lescouezec, R.; Vaissermann, J.; Toma, L. M.; Carrasco, R.; Lloret, F.; Julve, M. *Inorg. Chem.* **2004**, *43*, 2234. (h) Wang, S.; Zuo, J. L.; Zhou, H. C.; Choi, H. J.; Ke, Y.; Long, J. R.; You, X. Z. *Angew. Chem., Int. Ed.* **2004**, *43*, 5940.

(12) (a) Liu, T.; Dong, D. P.; Kanegawa, S.; Kang, S.; Sato, O.; Shiota, Y.; Yoshizawa, K.; Hayami, S.; Wu, S.; He, C.; Duan, C. Y. *Angew. Chem., Int. Ed.* **2012**, *51*, 4367. (b) Wen, H. R.; Tang, Y. Z.; Liu, C. M.; Chen, J. L.; Yu, C. L. *Inorg. Chem.* **2009**, *48*, 10177. (c) Senapati, T.; Pichon, C.; Ababei, R.; Mathoniere, C.; Clerac, R. *Inorg. Chem.* **2012**, *51*, 3796. (d) Kim, J. I.; Yoo, H. S.; Koh, E. K.; Kim, H. C.; Hong, C. S. *Inorg. Chem.* **2007**, *46*, 8481. (e) Kim, J. I.; Yoo, H. S.; Koh, E. K.; Hong, C. S. *Inorg. Chem.* **2007**, *46*, 10461. (f) Kim, J. L.; Kwak, H. Y.; Yoon, J. H.; Ryu, D. W.; Yoo, I. Y.; Yang, N.; Cho, B. K.; Park, J. G.; Lee, H.; Hong, C. S. *Inorg. Chem.* **2009**, *48*, 2956. (g) Li, F.; Clegg, J. K.; Goux-Capes, L.; Chastanet, G.; D'Alessandro, D. M.; Letard, J. F.; Kepert, C. J. *Angew. Chem., Int. Ed.* **2011**, *50*, 2820. (h) Jiang, L.; Choi, H. J.; Feng, X. L.; Lu, T. B.; Long, J. R. *Inorg. Chem.* **2007**, *46*, 2181. (i) Zhang, Y. J.; Liu, T.; Kanegawa, S.; Sato, O. *J. Am. Chem. Soc.* **2009**, *131*, 7942.

(13) (a) Panja, A.; Guionneau, P.; Jeon, I. R.; Holmes, S. M.; Clerac, R.; Mathoniere, C. *Inorg. Chem.* **2012**, *51*, 12350. (b) Jiang, L.; Feng, X. L.; Lu, T. B.; Gao, S. *Inorg. Chem.* **2006**, *45*, 5018. (c) Zhang, D. P.; Wang, H. L.; Chen, Y. T.; Zhang, L. F.; Tian, L. J.; Ni, Z. H.; Jiang, J. Z. *Dalton Trans.* **2009**, 9418. (d) Ni, Z. H.; Kou, H. Z.; Zhang, L. F.; Ni, W. W.; Jiang, Y. B.; Cui, A. L.; Ribas, J.; Sato, O. *Inorg. Chem.* **2005**, *44*, 9631. (e) Lescouezec, R.; Lloret, F.; Julve, M.; Vaissermann, J.; Verdaguer, M. *Inorg. Chem.* **2002**, *41*, 818. (f) Wang, S.; Zuo, J. L.; Zhou, H. C.; Song, Y.; Gao, S.; You, X. Z. *Eur. J. Inorg. Chem.* **2004**, 3681. (g) Hoshino, N.; Sekine, Y.; Nihei, M.; Oshio, H. *Chem. Commun.* **2010**, *46*, 6117. (h) Li, D.; Clerac, R.; Roubeau, O.; Harte, E.; Mathoniere, C.; Bris, R. L.; Holmes, S. M. *J. Am. Chem. Soc.* **2008**, *130*, 252. (i) Zhang, Y.; Li, D.; Clerac, R.; Kalisz, M.; Mathoniere, C.; Holmes, S. M. *Angew. Chem., Int. Ed.* **2010**, *49*, 3752.

(14) (a) Kim, J.; Han, S.; Cho, I. K.; Choi, K. Y.; Heu, M.; Yoon, S.; Suh, B. J. *Polyhedron* **2004**, *23*, 1333. (b) Wen, H. R.; Wang, C. F.; Zuo, J. L.; Song, Y.; Zeng, X. R.; You, X. Z. *Inorg. Chem.* **2006**, *45*, 582. (c) Kwak, H. Y.; Ryu, D. W.; Lee, J. W.; Yoon, J. H.; Kim, H. C.; Koh, E. K.; Krinsky, J.; Hong, C. S. *Inorg. Chem.* **2010**, *49*, 4632. (d) Wei, J.; Liang, X. Q.; Li, Y. Z.; Zuo, J. L.; You, X. Z. *Chin. J. Inorg. Chem.* **2007**, *23*, 473. (e) Wang, S.; Zuo, J. L.; Zhou, H. C.; Song, Y.; You, X. Z. *Inorg. Chim. Acta* **2005**, *358*, 2101. (f) Nihei, M.; Okamoto, Y.; Sekine, Y.; Hoshino, N.; Shiga, T.; Liu, I. P.; Oshio, H. *Angew. Chem., Int. Ed.* **2012**, *51*, 6361. (g) Siretanu, D.; Li, D.; Buisson, L.; Bassani, D. M.; Holmes, S. M.; Mathoniere, C.; Clerac, R. *Chem.—Eur. J.* **2011**, *17*, 11704. (h) Atanasov, M.; Comba, P.; Helmle, S. *Inorg. Chem.* **2012**, *51*, 9357. (i) Mondal, A.; Li, Y.; Herson, P.; Seuleiman, M.; Boillot, M. L.; Riviere, E.; Julve, M.; Rechignat, L.; Bousseksou, A.; Lescouezec, R. *Chem. Commun.* **2012**, *48*, 5653. (j) Zhang, Y. Z.; Mallik, U. P.; Rath, N. P.; Clerac, R.; Holmes, S. M. *Inorg. Chem.* **2011**, *50*, 10537.

(15) Miyasaka, H.; Saitoh, A.; Abec, S. *Coord. Chem. Rev.* **2007**, *251*, 2622.

(16) Przychodzeń, P.; Lewinski, K.; Balanda, M.; Pełka, R.; Rams, M.; Wasiutynshi, T.; Guyard-Duhayon, C.; Sieklucka, B. *Inorg. Chem.* **2004**, *43*, 2967.

(17) Przychodzeń, P.; Lewinski, K.; Balanda, M.; Pełka, R.; Rams, M.; Wasiutynshi, A. S.; McCann, M.; Casey, M. T.; Jackman, M.; Devereux, M.; McKee, V. *Inorg. Chem. Acta* **1988**, *279*, 24.

(18) Kahn, O. *Molecular Magnetism*; VCH: New York, 1993.

(19) *SMART, SAINT and XPREP: Area Detector Control and Data Integration and Reduction Software*; Bruker Analytical X-ray Instruments Inc.: Madison, WI, 1995.

(20) Sheldrick, G. M. *SADABS: Program for Empirical Absorption correction of Area Detector Data*; University of Göttingen: Göttingen, Germany, 1996.

(21) Sheldrick, G. M. *SHELXL-97: Program for the Refinement of Crystal Structure*; University of Göttingen: Göttingen, Germany, 1997.

(22) (a) Borras-Almenar, J. J.; Clemente-Juan, J. M.; Coronado, E.; Tsukerblat, B. *Inorg. Chem.* **1999**, *38*, 6081. (b) Borras-Almenar, J. J.; Clemente-Juan, J. M.; Coronado, E.; Tsukerblat, B. *MAGPACK, Magnetic Properties Analysis Package for Spin Clusters, version 00.1*; 2000. (c) Borras-Almenar, J. J.; Clemente-Juan, J. M.; Coronado, E.; Tsukerblat, B. *J. Comput. Chem.* **2001**, *22*, 985. (d) Zhou, H. B.; Wang, H. S.; Chen, Y.; Xu, Y. L.; Song, X. J.; Song, Y.; Zhang, Y. Q.; You, X. Z. *Dalton. Trans.* **2011**, *40*, 5999.

(23) Seiden, J. *J. Phys., Lett.* **1983**, *44*, L947.

(24) (a) Caneschi, A.; Gatteschi, D.; Melandri, M. C.; Rey, P.; Sessoli, R. *Inorg. Chem.* **1990**, *29*, 4228. (b) Chiari, B.; Cinti, A.; Piovesana, O.; Zanazzi, P. F. *Inorg. Chem.* **1995**, *34*, 2652. (c) Wrzeszcz, G.; Dobrzanska, L.; Wojtczak, A.; Grodzicki, A. *J. Chem. Soc., Dalton Trans.* **2002**, 2862.